UVB Irradiation-Induced Pain is Mediated by CXCL5

John M Dawes[1], Margarita Calvo[1*], James R Perkins[2*], Kathryn J Paterson[1*], Hannes Keisewetter[1], Carl Hobbs[1], Timothy KY Kaan[1], Christine Orengo[2], David LH Bennett[1,3], Stephen B McMahon[1]

[1] Wolfson Centre for Age Related Diseases, King's College London, London, SE1 1UL, United Kingdom.

[2] Department of Structural and Molecular Biology, University College London, London WC1E 6BT, United Kingdom.

[3] Department of Neurology King's College Hospital.

* M. Calvo, J.R. Perkins and K.J. Paterson contributed equally to this work.

Abstract

Many persistent pain states (pain lasting for hours, days or longer) are poorly treated because of the limitations of existing therapies such as NSAIDs and opioids. Identification of the key mediators of various types of pain could improve such therapies. Here we tested the hypothesis that hitherto unrecognized cytokines and chemokines might act as mediators in inflammatory pain. We used UVB-irradiation to induce persistent, abnormal sensitivity to pain in humans and rodents. The expression of over 90 different inflammatory mediators was measured in treated skin at the peak of UVB-induced hypersensitivity with custom-made PCR arrays. There was a significant positive correlation in the overall expression profiles between the two species. The expression of several genes (IL-1β, IL-6 and COX-2), previously shown to contribute to pain hypersensitivity, was significantly increased after UVB exposure and there was dysregulation of several chemokines. Among cytokines, CXCL5 was induced to the greatest extent by UVB treatment in human skin; when injected into the skin of rats, CXCL5 recapitulated the mechanical hypersensitivity caused by UVB irradiation. This hypersensitivity was associated with the infiltration of neutrophils and macrophages into the dermis, and neutralizing the effects of CXCL5 attenuated the abnormal pain-like behavior. Our findings demonstrate that the chemokine CXCL5 is a peripheral mediator of UVB-induced inflammatory pain.

Introduction

During inflammation, molecules such as hydrogen ions, purines, lipids (for example, prostanoids) and immune-related agents (cytokines and chemokines) can sensitize nociceptors (pain-sensitive cells), typically by the phosphorlyation of various intracellular kinases, and evoke hyperalgesia or increased sensitivity to noxious stimuli (1). Resident or infiltrating inflammatory cells such as macrophages, neutrophils, lymphocytes and mast cells can release a wide range of cytokines and chemokines, such as interleukin 1 beta (IL-1β), tumour necrosis factor alpha (TNFα) and nerve growth factor (NGF) (2,3), which induce and maintain pain-related hypersensitivity. In the skin, keratinocytes release cytokines after injury and during inflammation (4,5). Cytokines and chemokines are important in recruiting different types of immune cells and can themselves directly influence transduction mechanisms in nociceptors (6,7,8).

Despite this understanding, there are still few drugs for inflammatory pain that have made the transition from bench to bedside. One issue that has been blamed for this poor conversion rate is the over-dependency of the drug discovery process on animal models, in which factors such as species, strain and sex influence the ability of models to predict analgesia in human patients (9). Experiments on healthy human volunteers in which a defined injurious stimulus is followed by assessment of sensory processing can help to bridge this gap (10). In human studies, nociceptors can be activated directly by agents applied to skin, including ATP (11), capsaicin or mustard oil (12), thermal burn (13), freeze injury (14), histamine or cowhage (15) or irradiation with ultraviolet-B (UVB) light.

Inflammation from a UVB burn produces a robust dose-dependent hypersensitivity to thermal and mechanical stimulation in man and rodents, which peaks between 24 and 48 hours after irradiation (16,17,18,19). UVB-induced hypersensitivity is confined to the irradiated area in both species and does not depend on NMDA receptor recruitment (20). After a UVB burn, rat primary afferent nociceptors do not develop spontaneous activity but heat-insensitive C fibers show an enhanced response to suprathreshold mechanical stimuli, and heat-sensitive C fibers develop an increased response to noxious heat. These findings suggest that this extra-responsive pain state is induced by mediators acting peripherally (16,17,20). UVB-irradiation increases the expression of inflammatory mediators such as IL-1β, IL6 and IL-10 in vivo (21,22). Additionally, irradiation of cells in vitro, such as mast cells which are abundant in the skin, can up-regulate the mRNA for the major inflammatory chemokine CXCL8 (23). We used UVB irradiation as a stimulus to compare mediator expression in human and rat skin in a systematic fashion and to identify peripheral mediators of hyperalgesia With custom-made PCR array cards we measured transcripts from over 90 different putative inflammatory mediators at the peak of pain-related hypersensitivity in human and rat UVB irradiated skin.

Results

UVB irradiation causes sensory changes in human and rat skin

To compare the expression of cytokines and chemokines during UVB-induced inflammation in human and rat skin, we chose a level of irradiation known to result in increased blood flow as well as in mechanical and thermal pain-related hypersensitivity (16,17). We selected a time point of 40 hours after irradiation because sensory changes are known to peak between 1 and 2 days. In human forearm skin, three minimal-erythema doses (MEDs) of UVB applied to an area of 10 mm^2 caused a significant increase in blood flow to the irradiated area (230.1±29.2 arbitrary units (AU)) compared to a non-irradiated control skin site (14.4±3.2 AU) (Fig. 1A). In rats the plantar surface of the hind limb was irradiated with 1000mJ/cm^2 of UVB, also producing a significant increase in blood flow (169.7±25.8 AU) when compared to the contralateral limb's non-irradiated skin surface (39.3±4.4 AU) (Fig. 1B). A clear mechanical and thermal hyperalgesia was observed in both human and rat skin irradiated with UVB. The mean 50% pain threshold to mechanical stimulation was found to be 17.6±5.8 g in control skin from human volunteers. This was significantly reduced to 1.4±.03 g (Fig. 1C) within the irradiated area. Mean heat pain thresholds were also significantly reduced to 40.1±0.5 ^oC from 47.2±0.7 ^oC in non-irradiated skin (Fig 1E). In rats, UVB irradiation caused a significant drop in mechanical withdrawal thresholds from 11.2±1.5 g in the contralateral non-irradiated skin to 4.1±0.5 g in irradiated skin (Fig. 1D). Thermal withdrawal latencies were also significantly reduced from 14±0.5 s on the control side to 7.4±0.6 s in the irradiated site (Fig. 1F). Despite the use of general anaesthetics in the rats, which may have delayed the inflammatory process (24), the cardinal signs of inflammation were present, and these results demonstrate similarity in mechanical and thermal

hypersensitivity between the human and rat when equivalent doses of UVB are used (16,17).

UVB irradiation regulates inflammatory mediators

We designed custom-made Taqman Array cards to determine the expression of a large number of the inflammatory mediators (mainly chemokines and cytokines) in UVB-treated rat and human skin 40 hours after irradiation. Wherever possible, rat and human orthologs of the mediators were included to enable direct comparison between species. All data from rat and human cards are shown in Tables S1 and S2, respectively. Data are displayed as a fold change (FC) in the relative expression of the transcript in UVB, setting the value from control skin as 1.0. Table 1 shows the top 20 up-regulated transcripts, ranked by FC, in rat and human, a majority of which were statistically significant when compared to control. A number of transcripts with a known role in inflammatory hyperalgesia were up-regulated in both species. For example, IL-1β and the enzyme cyclooxygenase-2 (COX-2) were both significantly up-regulated (Rat: 5.0 (1.3-18.7) (FC (range)), 4.6 (2.0-10.6), Human: 10.3 (5.9-17.8), 5.3 (3.0-9.5) respectively) in both species. A number of other mediators exhibited even larger increases; many of these were chemokines (7 of the top 10 in Table 1). Of particular interest was the chemokine CXCL5, the top up-regulated transcript in both species (Rat: 51.3 (20.5-128.2), Human: 82.5 (45.4-150.0)). This chemokine has not previously been implicated in nociceptive processing but is elevated in certain chronic pain syndromes (25). Using the more readily available rat tissue, we confirmed both the up-regulation and significance levels for a number of the top up-regulated mediators (Fig. S1) using conventional Q-PCR. The results with

conventional Q-PCR were highly consistent with those obtained with Taqman array PCR, hence validating our array data.

UVB-induced gene changes are correlated in human and rat

73 out of the 92 different target transcripts detected were represented on Taqman array cards for the two species. By using an average of their FC in a log 2 format, we plotted UVB-induced gene changes from the human and rat against each other. Calculation of the Pearson's correlation coefficient ($r=0.435$) determined that there was an overall positive correlation between the two sets of data (Fig. 2). In addition, this relationship was significant ($p=0.00012$), suggesting that the inflammatory process induced by UVB irradiation and required for the development of thermal and mechanical hypersensitivity, was similar in both species. The concordance between the two models is further emphasised by comparison of the FC values from the mediators that showed the top transcriptional changes (Table 1). Nevertheless, there were some genes (Figure 2, triangles) that showed differential regulation in human and rat (CCL20, IL-1α, IL-20 and iNOS). When the distribution of the difference between the human and rat FC value for each gene was plotted, these four genes were situated 2 standard deviations away from the norm and therefore could be potential considered outliers. Without these four genes, there is positive shift in the Pearson's correlation coefficient, to $r=0.69$. Human volunteers consisted of both males and females, while only male rats were used for the PCR array. Because females have a higher incidence of some inflammatory diseases, we compared inflammatory mediator expression between genders and found a strong positive and highly significant correlation ($r=0.88$, $p<0.001$) (Fig. S2), justifying our direct comparison of the human data with the rat data.

The chemokine CXCL5 causes mechanical pain-related hypersensitivity and induces infiltration of neutrophils and macrophages.

CXCL5 expression was up-regulated at the peak of UVB-induced hypersensitivity in both species, 40 hours after UVB treatment. In addition the non-steriodal anti-inflammatory drug (NSAID) Piroxicam significantly attenuated the increased CXCL5 expression in the rat UVB model (Fig. S3). We know that UVB-induced hypersensitivity is susceptible to NSAID treatment (16,26), and therefore we next investigated the possible algogenic, or pain producing, role of this chemokine. Intra-plantar (I.pl.) injection of CXCL5 caused a dose-dependent reduction in mechanical pain thresholds at 0.5 (5.1±1.2 g) and 6 (5.7±0.9 g) hours after treatment when compared to vehicle control (10.4±1.4 g and 11.9±1.2 g, respectively) (Fig. 3A). Mechanical thresholds returned to baseline levels by 24 hours. In the same animals there was no significant alteration in thermal withdrawal latencies at any dose (Fig. 3B), compared to vehicle treated animals.

CXCL5, like all chemokines, can cause chemoattraction of certain immune cells, in particular neutrophils (27). Therefore we investigated whether its ability to induce pain-related mechanical hypersensitivity was associated with cellular infiltration into the skin. An H & E stain revealed the presence of both monocytes and polymorphonuclear (PMN) cells within the dermis 6 hours after injection of the chemokine (Fig. 3C&D).

By using an antibody against IBA1, a marker of cells from the monocyte lineage and hence macrophages (28), we found intense staining in rat skin 6 hours after CXCL5 treatment compared to vehicle (Fig. 3E&F). With Q-PCR we found that the increase in IBA1 staining was accompanied by a significant increase in the relative expression

of IBA1 mRNA in CXCL5 treated skin (2.7±0.5) compared to control (1.0±0.1) (Fig. 3I). Low levels of CD3, a pan T-cell marker, were detected in rat skin following vehicle and CXCL5 treatment (Fig. 3G&H) and no difference was measured using Q-PCR (Fig. 3J). To measure the levels of neutrophils using Q-PCR, we used primers against the granulocyte colony-stimulating factor receptor (G-CSFR). This receptor is primarily found on myeloblasts and mature neutrophils (29) and therefore, in skin, is a good marker of infiltrating PMN cells that have matured. In agreement with the H & E staining results, we found a significant increase in G-CSFR mRNA expression of 16.3±2.9 compared to vehicle treated skin (Fig. 3K). CXCL5 acts largely through the G-protein coupled receptor CXCR2 (26). This receptor is found primarily on neutrophils, but can also be expressed on macrophages and mast cells (30). After CXCL5 treatment, we also saw a significant increase in CXCR2 mRNA (Fig. L), possibly from infiltrating cells attracted by CXCL5, suggesting that this chemokine is acting in a receptor-specific manner.

UVB-induced hypersensitivity and CXCL5 expression peak at 48 hours

UVB irradiation causes a prolonged inflammatory pain state with pain-related hypersensitivity in the rat lasting for 10-14 days (16). Thresholds to mechanical stimulation were significantly reduced 24 and 48 hours after irradiation when compared to naïve animals, but had returned to normal by 10 days after irradiation (Fig. 4A). In the same animals, we saw a significant reduction in withdrawal latency to a heat stimulus 24 and 48 hours after UVB treatment when compared to naïve animals; withdrawal latency returned to normal by 10 days (Fig. 4B). We next measured the expression of CXCL5 in the irradiated skin taken from these animals. Compared to mRNA levels in naïve skin and in agreement with the Taqman array data (Table 1), CXCL5 was significantly up-regulated most prominently 48 hours

after irradiation with a relative mRNA expression of 339.6±171.6 versus control (1.0±0.3) (Fig. 4C). There was also more but non-significant expression at 24 hours (7.4±2.4) versus control. We also measured protein levels when CXCL5 mRNA expression was at its peak. In non-irradiated skin CXCL5 protein was not detected; however, 48 hours after UVB treatment a significant amount was seen in the inflamed skin (Fig. 4D). At the peak of pain-related hypersensitivity and CXCL5 expression (48 hours), we also measured macrophage, neutrophil and T cell makers. Compared to control, 48 hours after UVB treatment, skin showed a significant increase in IBA1 (2.8±0.7) and G-CSFR (32.7±11.1) mRNA expression, similar to that seen after CXCL5 treatment alone (Fig. 4E&G). We also see a small increase in CXCR2 expression (1.46±.25) compared to control (1.0±0.1). However, this was not significant. Again, no differences were measured in the expression CD3 (Fig. 4F), suggesting a lack of T-cell influence in UVB-induced inflammation. Because we used both genders in the human group and because the inflammatory response, particularly with regards to neutrophil attraction, shows sex-differences (31), we repeated these experiments in female rats. As in male rats, females showed a significant hypersensitivity 48 hours after UVB treatment. This was accompanied by significant increases in CXCL5, IBA1 and GCSFR mRNA expression, indicating a comparable inflammatory response in female rats (Fig. S4A-D).

Neutralisation of CXCL5 attenuates UVB-induced mechanical hypersensitivity and decreases the number of infiltrating cells

We next tested whether and to what extent CXCL5 contributes to the mechanical hypersensitivity caused by UVB treatment. In irradiated rats, repeated doses of a

neutralising antibody (Ab) against CXCL5 significantly attenuated the reduced mechanical withdrawal thresholds 30 hours after UVB irradiation (6.0±0.8g), when compared to the group receiving a control IgG Ab (3.6±0.7g) (Fig. 5A), while no difference between groups was observed for thermal hypersensitivity at any time point (Fig. 5B). The neutralisation of CXCL5 in the irradiated paw did not alter withdrawal thresholds or change the expression of IBA1 and GCSFR at the early 8 hour time point (Fig5. C&D). 30 hours after UVB irradiation, however, the attenuation of UVB-induced mechanical hypersensitivity was associated with a reduction in infiltrating macrophages and neutrophils. IBA1 staining was reduced in irradiated rat skin treated with the CXCL5 Ab compared to those treated with the IgG Ab (Fig. 5, I and K). This reduction was significant when measured by Q-PCR (Fig. 5E). Again very few cells were positively stained for CD3 (Fig. J&L), and no difference was measured in CD3 mRNA expression (Fig. 5F). Significant reductions in G-CSFR expression and CXCR2 were also measured after local neutralization of CXCL5 (Fig. 5G&H).

CXCL5 triggers calcium responses and increases migration in macrophages in vitro.

All chemokines bind to G-protein coupled receptors which, when activated, cause changes in intracellular calcium levels (32). We found that CXCL5 caused a calcium response in cultured macrophages (Fig. 6A-D). At a dose of 100nM, CXCL5 activated 43.3±5% of the macrophages, significantly more than vehicle (0%) (Fig. 6E). An example of this response is shown in Fig. 6F. 10nM of CXCL5 did not have an effect on calcium concentrations (Fig. 6E). No response was seen in sensory

neurons cultured from the dorsal root ganglia (DRG) (Fig. 6G), suggesting that CXCL5 does not directly activate this cell type.

CXCL5 promote chemotaxis of neutrophils (33,34); however, its chemotactic effects on macrophages have not been examined. Using a Boyden chamber, in which cells cross a concentration gradient through a porous filter, we found that a significantly increased percentage of macrophages migrated towards wells containing 1 (1392.7±133%) and 10nM (1142.9±239%) of CXCL5 over those containing control solution (100%) (Fig. 7A). The cells in control and CXCL5 (10nM) treated wells are shown in Figure 7B & C. To assess whether CXCL5 is a chemotactic or a chemokinetic factor, we used a checkerboard analysis (35). When the concentration of the chemokine was equal in both upper and lower wells, we noted enhanced migration as a result of increased motility in a non-directional manner, a process termed chemokinesis. However, when there was a concentration gradient between the upper and lower chambers migration was significantly higher, indicating that CXCL5 is a true chemotactic factor for macrophages (Fig. 7D).

Discussion

Quantified doses of UVB irradiation applied to small patches of skin induce a marked hyperalgesia with a parallel time course and magnitude in rats and humans (16,17,18,19). The mechanism of UVB-induced hyperalgesia is not definitively established, but a major component is the peripheral sensitization of nociceptive afferent terminals in the irradiated skin (20). The mediators driving this peripheral sensitization are themselves not defined, but anti-inflammatory drugs reduce the sensory sequelae of UVB irradiation (16, 21, 26).

First we used PCR to characterise the expression of inflammatory mediators in rat and human. PCR arrays are sensitive enough tor assess the expression of a large number of transcripts in small tissue samples, samples of a size that can be realistically obtainable in a clinical setting from a range of patient groups. Our arrays assessed the expression of a broad range of inflammatory mediators with a particular emphasis on cytokines and chemokines. At the peak of UVB-induced hypersensitivity (40 hours), in both humans and rats, a number of chemokines and cytokines were transcriptionally up-regulated. Angst et al (21) used microdialysis to assay the protein levels of a more restricted number of putative mediators 24 hours after UVB irradiationin human skin. As in our study, they found elevated levels of IL-6, IL-8, IL-10, G-CSF and CCL4, and no change in TNFα and NGF. In contrast to our results, however, they did not find a significant increase in CCL2 or IL-1β.

Our second aim was to increase the likelihood that our results could be translated to the clinic. Pain mechanisms have in the past largely been explored in animal models, some of which have an uncertain relationship to chronic pain states in patients, which has hampered clinical translation. Although there have been several efforts to

introduce animal models with greater face validity (e.g. chemotherapy-agent induced neuropathies in rodents (36,37)) there are still uncertainties about translatability across species. Our data demonstrate that after UVB irradiation, humans and rodents show transcriptional upregulation of similar genes. This significant correlation of gene expression between species was not necessarily expected because the immune response has been thought to be more species-specific than other mechanisms. We categorized the response of inflammatory mediators to UVB irradiation One group showed little alteration by UVB, changing less than two-foldand comprising about 50-60% of transcripts studied. A second group of about 15 factors was moderately up-regulated in both species and included several previously identified genes with known roles in pain modulation such as CCL2, CCL3, COX-2 and IL-1β. A small number of factors were dramatically up-regulated in both species by UVB treatment, and these are CXCL5, CXCL2, IL-24 and IL-6. Four factors were regulated in a discordantn manner between species.

The degree of correlation in gene expression suggested a similar underlying biological response, at least in terms of inflammatory mediators, in humans and rats at the peak of UVB-induced hypersensitivity. This Other persistent pain states in humans may also share mechanisms with rodents, which would facilitate the development of treatments. One example is osteoarthritis (OA) in which the majority of pain arises from peripheral tissues (38), driven by peripheral mediators. These mediators are unidentified and, although the animal models of OA show joint damage and sensory abnormalities, it is still not clear whether they do so by releasing the same mediators that drive OA pain in patients. The approach we describe here may help to identify the clinically relevant factors.

The highly upregulated transcripts by UVB have not been previously described as potential pain mediators. This group consisted mainly of chemokines: CCL4, CCL7, CCL11, CXCL2, CXCL5 and CXCL7, as well as the cytokine IL-24. The chemokine family has over 50 members, and our data support the notion that this family contains a relatively unexplored group of promising pain mediators. Two chemokines, CCL2 and CX3CL1, have been extensively studied in chronic pain, either due to their actions on glia cells (39,40,41) or in the case of CCL2 also via neuronal interactions (42,43). Other chemokines act peripherally. For example the individual I.pl. injection of several chemokines (CCL2, CCL22, CCL5, CXCL1, CXCL8 and CXCL12) induces pain-related hypersensitivity in normal rats (44,7,45). A number of these previously described pro-nociceptive chemokines were significantly up-regulated in our UVB model (CCL2, CXCL1 and CXCL8).

Our data on UVB-induced mechanical hypersensitivity points to a previously unrecognised role for the chemokine CXCL5. CXCL5, also known as epithelial-derived neutrophil activating peptide-78 in humans and lipopolysaccharide-induced CXC chemokine (LIX) in rodents, is involved in the recruitment and activation of leukocytes during inflammatory conditions (27). For example, this chemokine is elevated in the knee joints of arthritic patients and contributes to neutrophil recruitment (46). CXCL5 is one of a subclass of CXC chemokines that carry a glumate-leucine-arginine (ELR) motif and act mainly via the CXCR2 receptor, although it may also act through other receptors (47,48). The CXCR2 receptor is present on neutrophils, monocytes and endothelial cells and is important in neutrophil chemoattraction and monocyte arrest during inflammation (27). CXCL5 can be expressed by cells of the epidermis such as keratinocytes (49), as well as infiltrating monocytes (50), and it is likely that both of these cell types contribute to

the increased expression of CXCL5 after UVB irradiation. The non-selective COX inhibitor Piroxicam, like all NSAIDs, reduces inflammation in general and consequently has analgesic properties. At the peak of pain-related hypersensitivity, 48 hours after UVB treatment, the expression of CXCL5 mRNA was at its highest and could be partially ameliorated by Piroxicam treatment. In addition we also detect a significant level of CXCL5 protein at this time point. When injected into the plantar surface of the rat paw, CXCL5 evoked a mechanical but not thermal pain-related hypersensitivity. This hypersensitivity was associated with an infiltration of macrophages and neutrophils into the dermis. CXCL5 is a chemotactic agent for neutrophils (33,34). Our data show that CXCL5 elicits sizeable calcium responses in neutrophils and potently attracts cultured peritoneal macrophages

Irradiating the skin with UVB causes damage to DNA and apoptosis of epidermal cells (51). In mice, the subsequent inflammation results in recruitment of neutrophils and macrophages into the dermis (52,53). We found that blocking the action of CXCL5 in the UVB-treated rodent significantly reduced the levels of macrophages and neutrophils in the skin at the time of maximal mechanical hypersensitivity. CXCL5 is therefore likely to contribute to the sensory changes evoked by UVB irradiation through the recruitment of inflammatory cells and the subsequent release of proalgesic mediatorsBoth neutrophils and macrophages have been implicated in the development of abnormal pain states (54,55,56,57). Reduction of neutrophil recruitment attenuates pain-related hypersensitivity in some laboratory models of inflammation, for instance, in those associated with carrageenan and zymosan treatment (58,59). Other chemokines with the ability to attract neutrophils such as CXCL1, CXCL2, and CXCL8 (in humans), were also significantly up-regulated after UVB treatment. These molecules may also have contributed to the infiltration of PMN

cells and the subsequent sensory changes measured after UVB irradiation in our experiments. Pain-related hypersensitivity arising from nerve ligation or transection in rodents is partially dependent on macrophage recruitment (54,60). Other chemokines with the ability to attract macrophages such as CCL2, CCL3 and CCL7 were also up-regulated in UVB treated skin, suggesting that this cell type may also contribute to UVB-induced hypersensitivity

CXCL8 and CXCL1 are other members of the CXC chemokine family with ELR motifs that can induce pain-related hypersensitivity when injected peripherally (44,61). Both of these agents can act through the CXCR2 receptor. Antagonism of this receptor can attenuate pain-related hypersensitivity in a number of experimental pain states in rodents. These include the collagen-induced arthritis model, inflammatory pain arising from carrageenan, CFA or zymosan injection and neuropathic-like pain as a result of partial nerve injury (55,62). Attenuation of the hypersensitivity in these models, by CXCR2 blockade, is often associated with a decreased neutrophil infiltration.

There is a significant increase in mechanical pain-related hypersensitivity 0.5 hours after CXCL5 application, that is not associated with leukocyte infiltration. CXCL5 therefore may act either directly on nociceptive terminals or via other resident cells expressing CXCR2. We have not been able to demonstrate direct effects of CXCL5 on dissociated cultured DRG neurons using calcium imaging, although there is some data suggesting CXCR2 receptors are expressed in DRG cells (63). CXCL5 is however known to amplify the inflammatory cascade in endothelial cells, by activating NF-KappaB and increasing the expression of multiple pro-inflammatory mediators (64). CXCR2 receptors can also be expressed on mast cells and tissue

resident macrophages and, when activated with CXCL5, these cells can quickly release pro-algesic factors such as TNFα (30). The injection of CXCL1 and another ELR member, CXCL2, (both up-regulated in this study by UVB) do not evoke thermal or mechanical pain-related hypersensitivity despite PMN cell recruitment (65), suggesting that the pro-algesic properties of CXCL5 may be mediated through its action on resident or infiltrating macrophages.

Our studies demonstrate the utility of experimental pain models in animals and humans to understand pathophysiological mechanisms likely to be relevant in man. They underline the importance of inflammatory mediators, in particular the chemokines, in the development of abnormal pain states, emphasizing their significance as targets for the development of new analgesics.

Materials and Methods

Animals

Experiments were performed with male Wistar rats (~250g, Harlan) in accordance to the United Kingdom Home Office regulations. Food and water was available *ad libitum* and animals were housed under standard conditions with a 12 hour light/dark cycle.

Volunteers

A total of 10 healthy volunteers (6 male and 4 female) were used for the study. All volunteers had skin of either type II or III (66) as established via an initial screen. Individuals with known skin hypersensitivity, dermatological conditions such as eczema or dermatitis were excluded from all experiments. All participants were asked to refrain from analgesics, anti-inflammatory or anti-histamine medication for 4 hours prior to irradiation and until all testing was completed. Caffeine or nicotine was forbidden for 1 hour prior to psychophysical testing. This study was approved by the Ethics Committee of King's College London, and informed consent was obtained in writing from all participants.

UVB Irradiation

Rats were anaesthetised with a combination of medetomidine, Domitor (0.25mg/kg) and ketamine, Vetalar (60mg/kg) given i.p. When completely anaesthetised, rats were covered, exposing only the plantar surface of the hind paw or the depilated lower limb and placed under TL01 fluorescent bulbs with a maximum wavelength of 311nm. The irradiance output was measured by use of a photometer (IL1400A with SEL240/UVB-1/TD filter, ABLE Instruments & Controls) placed at the distance of the

exposed skin. This reading was used to calculate the time needed to deliver 1000mJ/cm^2 of UVB. Following the procedure and at least 45 minutes after anesthetisation animals were given an s.c. injection of atipamezole hydrochloride (1m/kg).

Volunteers received UVB irradiation at 3 times Mean Erythema Dose (MED) to an area of 10 mm^2 volar forearm using the TL01 fluorescent bulbs. The time to reach this dose was calculated from an initial screening protocol in which 1 MED was defined as the time needed to produce uniform reddening of the area 24 hours post irradiation. This involved irradiating 6 x 1cm^2 patches of volar forearm skin with varying doses, beginning at 307.5mJ/cm^2 and increasing the dose by 1.25mJ/cm^2 every square.

Behavioural testing

Mechanical hyperalgesia was assessed with the up-down method (67) by measuring withdrawal responses to a range of calibrated Von Frey hairs applied to the plantar surface of the rat hind paw. Thermal hyperalgesia was assessed by applying a radiant heat source to the same area and measuring the latency to withdrawal (68). For all behavioural experiments, rats were acclimatised for 1 week and baseline readings acquired. All behaviour was performed with the experimenter blind to treatment.

Psychophysical testing in humans

Mechanical pain thresholds were assessed in human volunteers by applying a range of calibrated Von Frey hairs of incremental force to the UVB treated volar forearm skin 40 hours after irradiation. The subject was asked to rate each stimulus as painful or not painful, and the up-down method was again applied to calculate their

50% withdrawal threshold. Heat pain threshold was derived as the arithmetic mean of three consecutive measurements with a Thermal Sensory Analyser (TSA 2001-II, MEDOC) thermode held against the skin (69). Thresholds were obtained using ramped stimuli (0.5°C/s), which terminated when the subject pressed a button to indicate first percept of pain. Temperature of the thermode ramped down to baseline temperature of 32°C (centre of neutral range) at a rate of ~5°C/s and remained at 32°C during 10s inter-stimulus interval. The contact area of the thermode was 10 mm². A maximal cut-off temperature of 50°C was employed whereby the TSA would automatically return to baseline temperature. Thermal testing was first demonstrated over an area that was not used for testing during the experiment.

Blood flow analysis

In both species blood flow to irradiated and unirradiated sites was measured with a laser Doppler flow meter (Moor-LAB, Moor instruments). Rats were anaesthetised and a Doppler probe placed on the skin surface of the depilated lower limb. In humans a similar probe was placed on the skin surface of the volar forearm. In both cases the average flux was calculated over a period of 15 seconds.

Tissue preparation and RNA extraction

Tissue samples, from irradiated and un-irradiated skin, were taken with the use of a biopsy punch (3.0mm, Stiefel) and immediately frozen in liquid nitrogen. In rats, samples were taken from depilated hairy skin of the lower hind limb. 3 mm punch biopsies were taken from control and irradiated skin in human volunteers. Skin samples were homogenised and total RNA obtained using a ‘hybrid’ method of phenol extraction (Trizol, Invitrogen) and column purification (RNeasy, Qiagen). This helped to achieve the extraction of high-quality RNA without a significant drop in

yield (All 260:280 A ratios were in the range of 1.94-2.13). All samples were DNase (Qiagen) treated to prevent genomic contamination. This was confirmed by using a RNA 6000 Nano Chip (Agilent) to ensure sufficient RNA integrity. RNA was subsequently synthesised into cDNA using the Superscript II reverse transcriptase kit (Invitrogen) and following the manufacturers protocol.

Taqman Array set-up and quantitative real-time PCR

Taqman array cards were custom made and designed using the Applied Biosystem website (70). Both human and rat 384 well cards were based on microfluidic technology and contained 4 sets of 96 different primer pairs which included 4 housekeeping genes (Glyceraldehyde 3-phosphate dehydrogenase (GAPDH), 18s, Beta-actin and Beta-2-microglobulin). Each cDNA sample was diluted with PCR grade water and added in a 1:1 ratio to Taqman Universal master mix producing a final concentration of 1ng/μl. Samples were fed into the appropriate loading ports (1μl for each well) and prepared according to the manufacturer's guidelines. Cards were placed into a 7900HT Fast Real-Time PCR system (Applied Biosystems) and cDNA samples were subjected to 40 cycles of amplification. Expression of each transcript was measured using the delta delta (ΔΔ)Ct (cycling time) method (71) normalised to the geometric mean of the 4 housekeeping genes using the R package NormqPCR (https://r-forge.r-project.org/projects/qpcr/) . Relative changes in transcript levels are presented as fold change (FC=UVB/Control). Where transcript numbers were undetermined for a given detector in less than 50% of samples, the average Ct value was calculated using the remaining data values. Where transcript numbers were undetermined in over 50% of transcripts for a given sample type (i.e.

case or control), the sample was given a default Ct of 38. If this occurred in both, no FC value was calculated.

For validation of UVB-induced gene changes and relative changes in the expression of cell markers, individual Q-PCR was performed using the Corbett Rotor-Gene 6000. Samples were processed in duplicate and amplified using the Roche lightcycler mastermix containing SYBR green for the detection of real-time changes. The efficiency of all primers was in the range of 0.8-1.2. Relative transcriptional expression was measured again using the (ΔΔ) Ct method normalised against GAPDH. Primers pairs were designed using the Primer Blast software (72), expect for CD3 (73) and are shown in the Table 1.

Detection of CXCL5 protein by ELISA

We used the Rat CXCL5/LIX DuoSet ELISA kit (detection range: 62.5-4000 pg/mL, DY543, R&D Systems) to detect the presence of CXCL5 protein in rat skin. Protein was extracted from depilated hairy skin by mechanical homogenisation in NP40 lysis buffer (20 mM Tris, pH 8, 137 mM NaCl, 10% glycerol, 1% NP-40, 2 mM EDTA), 20 μM leupeptin, 5 mM sodium fluoride, 1 mM sodium orthovanadate, 1 mM PMSF and protease inhibitor cocktail). Recombinant rat CXCL5/LIX standards and 5mg/ml of protein lysate were run in duplicate according to the manufacturer's instructions. Samples were read at 450 nm with wavelength correction at 540 nm. A reading within the range of the standard curve was considered positive and quantified. Protein was extracted from the ipsilateral and contralateral hairy skin of male Wistar rats 48 hours after being irradiated with 1000mJ/cm^2 of UVB light.

Histology

Rats were transaortically perfused with cold physiological saline and the plantar skin, to the depth of the hypodermis, was removed and placed in 4% paraformaldehyde overnight. The tissue was embedded in paraffin and 6 µm sections cut. The presence of inflammatory cells was determined using the counterstain Haematoxilyn and Eosin (H & E). Other sections were incubated with primary antibodies against ionised calcium binding adaptor molecule 1 (IBA1, Wako, 1:1000) and CD3 (Dakocytomation 1:3000) to detect the presence of macrophages and T-cells respectively. Briefly, sections were dewaxed and hydrated using a serial alcohol dilution. Endogenous peroxidases were inhibited with 3% H_20_2 and the mounted sections washed in buffer. Once blocked, sections were incubated with primary antibody for 2 hours. Following further wash steps, sections were incubated with a goat anti-rabbit biotinylated secondary antibody (Vectorlab, 1:300) for 30 minutes. Specific binding of the primary antibody was revealed using the vectorstain ABC kit (VectorLaboratories) with DAB.

Drug treatment

Animals were randomized into treatment groups and received I.pl. injections of either vehicle (PBS, 0.1% BSA), 0.1 µg, 1 µg or 3 µg of recombinant rat CXCL5/LIX (R & D Systems,), respectively, in a volume of 50 µl using a 0.3 ml insulin syringe (TERUMO, USA). Mechanical and thermal thresholds were measured in the treated skin at 0.5, 3, 6 and 24 hours post chemokine injection.

To evaluate the effects of a CXCL5 antibody on UVB irradiation rats received a 1000mJ/cm^2 dose of UVB to the plantar surface of the left hind paw. Immediately after irradiation an I.pl. injection of either a function blocking goat anti-rat CXCL5/LIX

antibody (R & D Systems) or normal goat IgG (R & D Systems) was given at a dose of 10 µg in 50 µl. Further antibody treatment was given directly after assessment of mechanical thresholds. Behaviour was carried out 8, 20 and 30 hours after UVB. The area of skin receiving treatment was taken for RNA extraction and histological assessment.

In vitro assays

Macrophage culture

Adult rats were killed using CO_2 and 20-50ml of sterile HBBS was injected into the peritoneal cavity. After 5 minutes the buffer was retrieved from the cavity and spun to obtain a cell pellet. Cells were resuspended in DMEM with 10% FBS and incubated at 37^{o}.

Calcium imaging

For calcium imaging cultured macrophages were incubated for 60-90 minutes at 37°C with 2µM Ca^{2+} indicator Fura2-AM (Invitrogen) in Hank's buffered salt solution (HBSS). Cells were transferred to a perfusion system attached to an inverted microscope (Nikon) equipped with a monochromator (Photon Technology). Recordings were carried out using a standardized protocol. Average Ca^{2+} concentration based fluorescent ratios (340/380nm excitation) were taken over the first 2 minutes of each run under continuous perfusion (3ml/min) with HBSS buffer solution (containing 10mM HEPES, pH 7.4) and defined as the baseline level. A single manual application of CXCL5 was followed by 3 minutes without continuous perfusion. After a 2 minute washout period, 25µM ATP (Sigma) or 20mM KCL were used as a positive control to define viable macrophages or dorsal root ganglion neurons (DRG) respectively. DRG neurons were cultured as previously described

(74). HBSS perfusion buffer for recordings with DRG neurons contained 10mM HEPES and 15mM glucose. All experiments were conducted at room temperature. Ratiometric changes of the 340/380nm wavelengths after manual application were normalized to the averaged baseline ratio. To be defined as a responder, cells needed a ratio change greater than 20% from baseline and a positive response to the application of ATP (macrophages) or KCL (DRG neurons).

Chemotaxis

To assess chemotactic ability the Boyden Chamber (Neuroprobe) was used. Briefly, varying concentrations of CXCL5, diluted in serum-free DMEM, was placed into the lower wells. Macrophages were suspended in serum-free DMEM and placed into the relevant top wells (50,000/well). A polycarbonate filter containing 5 μm pores was used to separate the wells. After 3 hours in the incubator at 37^{o} the membrane was removed and cells from the top wiped away. Cells which had migrated to the chemokine side were stained using RapiDiffII (Biostain Ready Reagents), membranes were coverslipped and cells counted.

Statistical analysis

For Taqman array cards, statistical significance was calculated by running t-tests in R (two-sided, Welch's t-test) on the ΔCt values. To control for multiple hypothesis testing, the p.values were adjusted using the false discovery rate (FDR) correction as proposed by Benjamini and Hochberg (75). All other statistical analysis was carried out using the SigmaStat software. Where the data was not normally distributed and had unequal variance, non-parametric tests were used.

Supplementary Material:

References and Notes

1. C.J. Woolf, Q. Ma, Nociceptors--noxious stimulus detectors, *Neuron* **55**, 353-364 (2007).
2. H.L. Rittner, H. Machelska, C. Stein, Leukocytes in the regulation of pain and analgesia, *J Leukoc Biol* **78**, 1215-1222 (2005).
3. W.A. Verri, Jr., T.M. Cunha, C.A. Parada, S. Poole, F.Q. Cunha, S.H. Ferreira, Hypernociceptive role of cytokines and chemokines: targets for analgesic drug development?, *Pharmacol Ther* **112**, 116-138 (2006).
4. C. Albanesi, P.O. De, G. Girolomoni, Resident skin cells in psoriasis: a special Look at the pathogenetic functions of keratinocytes, *Clin Dermatol* **25**, 581-588 (2007).
5. S. Pastore, F. Mascia, G. Girolomoni, The contribution of keratinocytes to the pathogenesis of atopic dermatitis, *Eur J Dermatol* **16**, 125-131 (2006).
6. A.M. Binshtok, H. Wang, K. Zimmermann, F. Amaya, D. Vardeh, L. Shi, G.J. Brenner, R.R. Ji, B.P. Bean, C.J. Woolf, T.A. Samad, Nociceptors are interleukin-1beta sensors, *J Neurosci* **28**, 14062-14073 (2008).
7. S.B. Oh, P.B. Tran, S.E. Gillard, R.W. Hurley, D.L. Hammond, R.J. Miller, Chemokines and glycoprotein120 produce pain hypersensitivity by directly exciting primary nociceptive neurons, *J Neurosci* **21**, 5027-5035 (2001).
8. N. Zhang, S. Inan, A. Cowan, R. Sun, J.M. Wang, T.J. Rogers, M. Caterina, J.J. Oppenheim, A proinflammatory chemokine, CCL3, sensitizes the heat- and capsaicin-gated ion channel TRPV1, *Proc Natl Acad Sci U S A* **102**, 4536-4541 (2005).
9. J.S. Mogil, Animal models of pain: progress and challenges, *Nat Rev Neurosci* **10**, 283-294 (2009).
10. M. Schmelz, Translating nociceptive processing into human pain models, *Exp Brain Res* **196**, 173-178 (2009).

11. A.A. Coutts, J.L. Jorizzo, R.A. Eady, M.W. Greaves, G. Burnstock, Adenosine triphosphate-evoked vascular changes in human skin: mechanism of action, *Eur J Pharmacol* **76**, 391-401 (1981).
12. M. Koltzenburg, L.E. Lundberg, H.E. Torebjork, Dynamic and static components of mechanical hyperalgesia in human hairy skin, *Pain* **51**, 207-219 (1992).
13. J.L. Pedersen, H. Kehlet, Hyperalgesia in a human model of acute inflammatory pain: a methodological study, *Pain* **74**, 139-151 (1998).
14. S. Kilo, M. Schmelz, M. Koltzenburg, H.O. Handwerker, Different patterns of hyperalgesia induced by experimental inflammation in human skin, *Brain* **117 (Pt 2)**, 385-396 (1994).
15. P. Sikand, S.G. Shimada, B.G. Green, R.H. Lamotte, Similar itch and nociceptive sensations evoked by punctate cutaneous application of capsaicin, histamine and cowhage, *Pain* **144**, 66-75 (2009).
16. T. Bishop, D.W. Hewson, P.K. Yip, M.S. Fahey, D. Dawbarn, A.R. Young, S.B. McMahon, Characterisation of ultraviolet-B-induced inflammation as a model of hyperalgesia in the rat, *Pain* **131**, 70-82 (2007).
17. T. Bishop, A. Ballard, H. Holmes, A.R. Young, S.B. McMahon, Ultraviolet-B induced inflammation of human skin: characterisation and comparison with traditional models of hyperalgesia, *Eur J Pain* **13**, 524-532 (2009).
18. G.I. Harrison, A.R. Young, S.B. McMahon, Ultraviolet radiation-induced inflammation as a model for cutaneous hyperalgesia, *J Invest Dermatol* **122**, 183-189 (2004).
19. R.T. Hoffmann, M. Schmelz, Time course of UVA- and UVB-induced inflammation and hyperalgesia in human skin, *Eur J Pain* **3**, 131-139 (1999).
20. T. Bishop, F. Marchand, A.R. Young, G.R. Lewin, S.B. McMahon, Ultraviolet-B-induced mechanical hyperalgesia: A role for peripheral sensitisation, *Pain* **150**, 141-152 (2010).

21. M.S. Angst, J.D. Clark, B. Carvalho, M. Tingle, M. Schmelz, D.C. Yeomans, Cytokine profile in human skin in response to experimental inflammation, noxious stimulation, and administration of a COX-inhibitor: a microdialysis study, *Pain* **139**, 15-27 (2008).
22. N.E. Saade, I.W. Nasr, C.A. Massaad, B. Safieh-Garabedian, S.J. Jabbur, S.A. Kanaan, Modulation of ultraviolet-induced hyperalgesia and cytokine upregulation by interleukins 10 and 13, *Br J Pharmacol* **131**, 1317-1324 (2000).
23. I. Endoh, G.N. Di, T. Hampartzoumian, B. Cameron, C.L. Geczy, N. Tedla, Ultraviolet B irradiation selectively increases the production of interleukin-8 in human cord blood-derived mast cells, *Clin Exp Immunol* **148**, 161-167 (2007).
24. J.M. Fuentes, M.A. Talamini, W.B. Fulton, E.J. Hanly, A.R. Aurora, M.A. De, General anesthesia delays the inflammatory response and increases survival for mice with endotoxic shock, *Clin Vaccine Immunol* **13**, 281-288 (2006).
25. W.W. Hochreiter, R.B. Nadler, A.E. Koch, P.L. Campbell, M. Ludwig, W. Weidner, A.J. Schaeffer, Evaluation of the cytokines interleukin 8 and epithelial neutrophil activating peptide 78 as indicators of inflammation in prostatic secretions, *Urology* **56**, 1025-1029 (2000).
26. T. Sycha, B. Gustorff, S. Lehr, A. Tanew, H.G. Eichler, L. Schmetterer, A simple pain model for the evaluation of analgesic effects of NSAIDs in healthy subjects, *Br J Clin Pharmacol* **56**, 165-172 (2003).
27. I.F. Charo, R.M. Ransohoff, The many roles of chemokines and chemokine receptors in inflammation, *N Engl J Med* **354**, 610-621 (2006).
28. M. Calvo, N. Zhu, C. Tsantoulas, Z. Ma, J. Grist, J.A. Loeb, D.L. Bennett, Neuregulin-ErbB signaling promotes microglial proliferation and chemotaxis contributing to microgliosis and pain after peripheral nerve injury, *J Neurosci* **30**, 5437-5450 (2010).
29. G.D. Demetri, J.D. Griffin, Granulocyte colony-stimulating factor and its receptor,

Blood **78**, 2791-2808 (1991).

30. S.M. Vieira, H.P. Lemos, R. Grespan, M.H. Napimoga, D. Dal-Secco, A. Freitas, T.M. Cunha, W.A. Verri, Jr., D.A. Souza-Junior, M.C. Jamur, K.S. Fernandes, C. Oliver, J.S. Silva, M.M. Teixeira, F.Q. Cunha, A crucial role for TNF-alpha in mediating neutrophil influx induced by endogenously generated or exogenous chemokines, KC/CXCL1 and LIX/CXCL5, *Br J Pharmacol* **158**, 779-789 (2009).
31. C.C. de, R.W. Gear, P.F. Dazin, H.Y. Sroussi, P.G. Green, J.D. Levine, Beta 2-adrenergic receptor regulation of human neutrophil function is sexually dimorphic, *Br J Pharmacol* **143**, 1033-1041 (2004).
32. T.D. Werry, G.F. Wilkinson, G.B. Willars, Mechanisms of cross-talk between G-protein-coupled receptors resulting in enhanced release of intracellular Ca2+, *Biochem J* **374**, 281-296 (2003).
33. A.M. Tester, J.H. Cox, A.R. Connor, A.E. Starr, R.A. Dean, X.S. Puente, C. Lopez-Otin, C.M. Overall, LPS responsiveness and neutrophil chemotaxis in vivo require PMN MMP-8 activity, *PLoS One* **2**, 312 (2007).
34. A. Walz, R. Burgener, B. Car, M. Baggiolini, S.L. Kunkel, R.M. Strieter, Structure and neutrophil-activating properties of a novel inflammatory peptide (ENA-78) with homology to interleukin 8, *J Exp Med* **174**, 1355-1362 (1991).
35. Y. Martinet, N. Martinet, J.M. Vignaud, F. Plenat, Blood monocyte chemotaxis, *J Immunol Methods* **174**, 209-214 (1994).
36. R.C. Polomano, A.J. Mannes, U.S. Clark, G.J. Bennett, A painful peripheral neuropathy in the rat produced by the chemotherapeutic drug, paclitaxel, *Pain* **94**, 293-304 (2001).
37. K.D. Tanner, D.B. Reichling, J.D. Levine, Nociceptor hyper-responsiveness during vincristine-induced painful peripheral neuropathy in the rat, *J Neurosci* **18**, 6480-6491 (1998).
38. G. Hawker, J. Wright, P. Coyte, J. Paul, R. Dittus, R. Croxford, B. Katz, C.

Bombardier, D. Heck, D. Freund, Health-related quality of life after knee replacement, *J Bone Joint Surg Am* **80**, 163-173 (1998).

39. A.K. Clark, P.K. Yip, J. Grist, C. Gentry, A.A. Staniland, F. Marchand, M. Dehvari, G. Wotherspoon, J. Winter, J. Ullah, S. Bevan, M. Malcangio, Inhibition of spinal microglial cathepsin S for the reversal of neuropathic pain, *Proc Natl Acad Sci U S A* **104**, 10655-10660 (2007).
40. M.A. Thacker, A.K. Clark, T. Bishop, J. Grist, P.K. Yip, L.D. Moon, S.W. Thompson, F. Marchand, S.B. McMahon, CCL2 is a key mediator of microglia activation in neuropathic pain states, *Eur J Pain* **13**, 263-272 (2009).
41. J. Zhang, X.Q. Shi, S. Echeverry, J.S. Mogil, K.Y. De, S. Rivest, Expression of CCR2 in both resident and bone marrow-derived microglia plays a critical role in neuropathic pain, *J Neurosci* **27**, 12396-12406 (2007).
42. Y.J. Gao, L. Zhang, O.A. Samad, M.R. Suter, K. Yasuhiko, Z.Z. Xu, J.Y. Park, A.L. Lind, Q. Ma, R.R. Ji, JNK-induced MCP-1 production in spinal cord astrocytes contributes to central sensitization and neuropathic pain, *J Neurosci* **29**, 4096-4108 (2009).
43. H. Jung, S. Bhangoo, G. Banisadr, C. Freitag, D. Ren, F.A. White, R.J. Miller, Visualization of chemokine receptor activation in transgenic mice reveals peripheral activation of CCR2 receptors in states of neuropathic pain, *J Neurosci* **29**, 8051-8062 (2009).
44. F.Q. Cunha, B.B. Lorenzetti, S. Poole, S.H. Ferreira, Interleukin-8 as a mediator of sympathetic pain, *Br J Pharmacol* **104**, 765-767 (1991).
45. X. Qin, Y. Wan, X. Wang, CCL2 and CXCL1 trigger calcitonin gene-related peptide release by exciting primary nociceptive neurons, *J Neurosci Res* **82**, 51-62 (2005).
46. R. Grespan, S.Y. Fukada, H.P. Lemos, S.M. Vieira, M.H. Napimoga, M.M. Teixeira, A.R. Fraser, F.Y. Liew, I.B. McInnes, F.Q. Cunha, CXCR2-specific

chemokines mediate leukotriene B4-dependent recruitment of neutrophils to inflamed joints in mice with antigen-induced arthritis, *Arthritis Rheum* **58**, 2030-2040 (2008).

47. H.R. Luttichau, The cytomegalovirus UL146 gene product vCXCL1 targets both CXCR1 and CXCR2 as an agonist, *J Biol Chem* **285**, 9137-9146 (2010).
48. E. Smith, H.M. McGettrick, M.A. Stone, J.S. Shaw, J. Middleton, G.B. Nash, C.D. Buckley, R.G. Ed, Duffy antigen receptor for chemokines and CXCL5 are essential for the recruitment of neutrophils in a multicellular model of rheumatoid arthritis synovium, *Arthritis Rheum* **58**, 1968-1973 (2008).
49. K. Boniface, F.X. Bernard, M. Garcia, A.L. Gurney, J.C. Lecron, F. Morel, IL-22 inhibits epidermal differentiation and induces proinflammatory gene expression and migration of human keratinocytes*, J Immunol* **174**, 3695-3702 (2005).
50. A. Walz, P. Schmutz, C. Mueller, S. Schnyder-Candrian, Regulation and function of the CXC chemokine ENA-78 in monocytes and its role in disease, *J Leukoc Biol* **62**, 604-611 (1997).
51. Y. Matsumura, H.N. Ananthaswamy, Toxic effects of ultraviolet radiation on the skin, *Toxicol Appl Pharmacol* **195**, 298-308 (2004).
52. M.L. Paz, A. Ferrari, F.S. Weill, J. Leoni, D.H. Maglio, Time-course evaluation and treatment of skin inflammatory immune response after ultraviolet B irradiation, *Cytokine* **44**, 70-77 (2008).
53. E. Toichi, K.Q. Lu, A.R. Swick, T.S. McCormick, K.D. Cooper, Skin-infiltrating monocytes/macrophages migrate to draining lymph nodes and produce IL-10 after contact sensitizer exposure to UV-irradiated skin, *J Invest Dermatol* **128**, 2705-2715 (2008).
54. J. Barclay, A.K. Clark, P. Ganju, C. Gentry, S. Patel, G. Wotherspoon, F. Buxton, C. Song, J. Ullah, J. Winter, A. Fox, S. Bevan, M. Malcangio, Role of the cysteine protease cathepsin S in neuropathic hyperalgesia, *Pain* **130**, 225-234 (2007).

55. T.M. Cunha, M.M. Barsante, A.T. Guerrero, W.A. Verri, Jr., S.H. Ferreira, F.M. Coelho, R. Bertini, G.C. Di, M. Allegretti, F.Q. Cunha, M.M. Teixeira, Treatment with DF 2162, a non-competitive allosteric inhibitor of CXCR1/2, diminishes neutrophil influx and inflammatory hypernociception in mice, *Br J Pharmacol* **154**, 460-470 (2008).
56. T.M. Cunha, W.A. Verri, Jr., I.R. Schivo, M.H. Napimoga, C.A. Parada, S. Poole, M.M. Teixeira, S.H. Ferreira, F.Q. Cunha, Crucial role of neutrophils in the development of mechanical inflammatory hypernociception, *J Leukoc Biol* **83**, 824-832 (2008).
57. J.D. Levine, J. Gooding, P. Donatoni, L. Borden, E.J. Goetzl, The role of the polymorphonuclear leukocyte in hyperalgesia, *J Neurosci* **5**, 3025-3029 (1985).
58. E. Ting, A.T. Guerrero, T.M. Cunha, W.A. Verri, Jr., S.M. Taylor, T.M. Woodruff, F.Q. Cunha, S.H. Ferreira, Role of complement C5a in mechanical inflammatory hypernociception: potential use of C5a receptor antagonists to control inflammatory pain, *Br J Pharmacol* **153**, 1043-1053 (2008).
59. Z.Z. Xu, L. Zhang, T. Liu, J.Y. Park, T. Berta, R. Yang, C.N. Serhan, R.R. Ji, Resolvins RvE1 and RvD1 attenuate inflammatory pain via central and peripheral actions, *Nat Med* **16**, 592-7 (2010).
60. R.R. Myers, H.M. Heckman, M. Rodriguez, Reduced hyperalgesia in nerve-injured WLD mice: relationship to nerve fiber phagocytosis, axonal degeneration, and regeneration in normal mice, *Exp Neurol* **141**, 94-101 (1996).
61. B.B. Lorenzetti, F.H. Veiga, C.A. Canetti, S. Poole, F.Q. Cunha, S.H. Ferreira, Cytokine-induced neutrophil chemoattractant 1 (CINC-1) mediates the sympathetic component of inflammatory mechanical hypersensitivitiy in rats, *Eur Cytokine Netw* **13**, 456-461 (2002).
62. M.N. Manjavachi, N.L. Quintao, M.M. Campos, I.K. Deschamps, R.A. Yunes, R.J. Nunes, P.C. Leal, J.B. Calixto, The effects of the selective and non-peptide

CXCR2 receptor antagonist SB225002 on acute and long-lasting models of nociception in mice, *Eur J Pain* **14**, 23-31 (2010).

63. J.G. Wang, J.A. Strong, W. Xie, R.H. Yang, D.E. Coyle, D.M. Wick, E.D. Dorsey, J.M. Zhang, The chemokine CXCL1/growth related oncogene increases sodium currents and neuronal excitability in small diameter sensory neurons, *Mol Pain* **4**, 38 (2008).
64. B. Chandrasekar, P.C. Melby, H.M. Sarau, M. Raveendran, R.P. Perla, F.M. Marelli-Berg, N.O. Dulin, I.S. Singh, Chemokine-cytokine cross-talk. The ELR+ CXC chemokine LIX (CXCL5) amplifies a proinflammatory cytokine response via a phosphatidylinositol 3-kinase-NF-kappa B pathway, *J Biol Chem* **278**, 4675-4686 (2003).
65. H.L. Rittner, S.A. Mousa, D. Labuz, K. Beschmann, M. Schafer, C. Stein, A. Brack, Selective local PMN recruitment by CXCL1 or CXCL2/3 injection does not cause inflammatory pain, *J Leukoc Biol* **79**, 1022-1032 (2006).
66. S. Astner, R.R. Anderson, Skin phototypes 2003, *J Invest Dermatol* **122**, 1-2 (2004).
67. S.R. Chaplan, F.W. Bach, J.W. Pogrel, J.M. Chung, T.L. Yaksh, Quantitative assessment of tactile allodynia in the rat paw, *J Neurosci Methods* **53**, 55-63 (1994).
68. K. Hargreaves, R. Dubner, F. Brown, C. Flores, J. Joris, A new and sensitive method for measuring thermal nociception in cutaneous hyperalgesia, *Pain* **32**, 77-88 (1988).
69. H. Fruhstorfer, U. Lindblom, W.C. Schmidt, Method for quantitative estimation of thermal thresholds in patients, *J Neurol Neurosurg Psychiatry* **39**, 1071-1075 (1976).
70. www.appliedbiosystems.com
71. T.D. Schmittgen, K.J. Livak, Analyzing real-time PCR data by the comparative

C(T) method, *Nat Protoc* **3**, 1101-1108 (2008).

72. http://www.ncbi.nlm.nih.gov/tools/primer-blast/

73. M. Costigan, A. Moss, A. Latremoliere, C. Johnston, M. Verma-Gandhu, T.A. Herbert, L. Barrett, G.J. Brenner, D. Vardeh, C.J. Woolf, M. Fitzgerald, T-cell infiltration and signaling in the adult dorsal spinal cord is a major contributor to neuropathic pain-like hypersensitivity, *J Neurosci* **29**, 14415-14422 (2009).

74. L.F. Wong, P.K. Yip, A. Battaglia, J. Grist, J. Corcoran, M. Maden, M. Azzouz, S.M. Kingsman, A.J. Kingsman, N.D. Mazarakis, S.B. McMahon, Retinoic acid receptor beta2 promotes functional regeneration of sensory axons in the spinal cord, *Nat Neurosci* **9**, 243-250 (2006).

75. Y. Benjamini, D. Drai, G. Elmer, N. Kafkafi, I. Golani, Controlling the false discovery rate in behavior genetics research, *Behav Brain Res* **125**, 279-284 (2001).

76. **Funding**: S.B.M. and D.L.H.B. are members of the Wellcome Trust-funded London Pain Consortium. D.L.H.B. is a Wellcome Trust Clinical Scientist. J.M.D. is funded by the Biotechnology and Biological Sciences Research Council and has a case studentship with AstraZeneca. M.C. is sponsored by the Chilean National Scholarship Program for Graduate Studies. J.R.P., K.J.P. and H.K., are students of the London Pain Consortium and funded by the Wellcome Trust. T.K.Y.K is the recipient of the National Sciences and Engineering Research Council of Canada (NSERC) postgraduate scholarship, Queen Elizabeth II Centennial Scholarship (Ministry of Advanced Education, British Columbia), and the Overseas Research Student Award (Universities UK). **Contributions:** S.B.M. and D.L.H.B. conceived of and coordinated the work presented. J.M.D. performed animal surgery, processed tissue, ran Taqman array cards and Q-PCRs. K.J.P. performed psychophysical testing on human volunteers**.** J.M.D. and T.K.Y. Kaan performed

animal behavioural testing**.** J.M.D. and J.R.P. carried out the analysis of PCR array data. C.O. provided information on PCR array analysis. M.C. cultured macrophages and performed chemotaxis experiments. H.K. cultured macrophages and performed calcium imaging experiments. C.H. performed Immunohistochemistry. S.B.M., D.L.H.B and J.M.D. wrote the manuscript**.** **Competing Interests**: The authors declare that they have no competing interests.

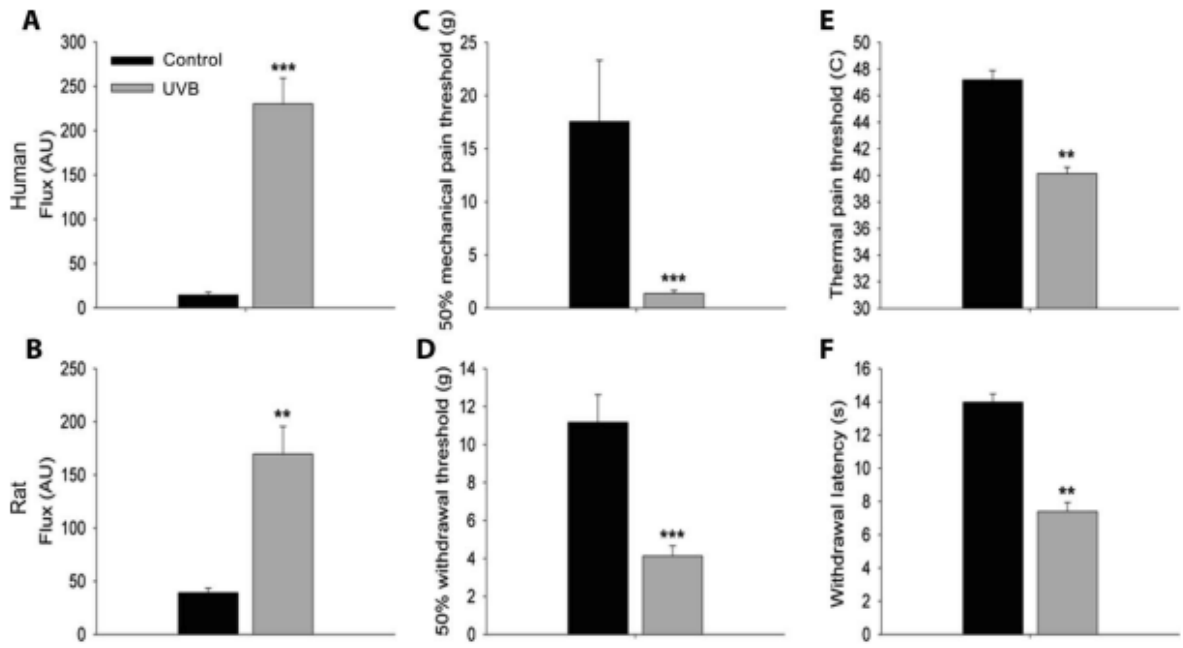

Figure 1. UVB-induced sensory changes in human and rat skin, 40 hours after UVB irradiation. (A, B) 3 MEDs and 1000mJ/cm^2 of UVB to human and rat skin, respectively, caused a significant increase in blood flow to the irradiated area when compared to control skin sites. (C-F) In the same area UVB-irradiation caused a significant reduction in thresholds to mechanical (C,D) and thermal (E,F) stimulation in human and rat skin, respectively (Paired t-test or Wilcoxon signed rank test (depending on data distribution), A, C, E, n=10. B, D, F, n=8, **p<0.01, ***p<0.001). All data is presented as the mean±SEM.

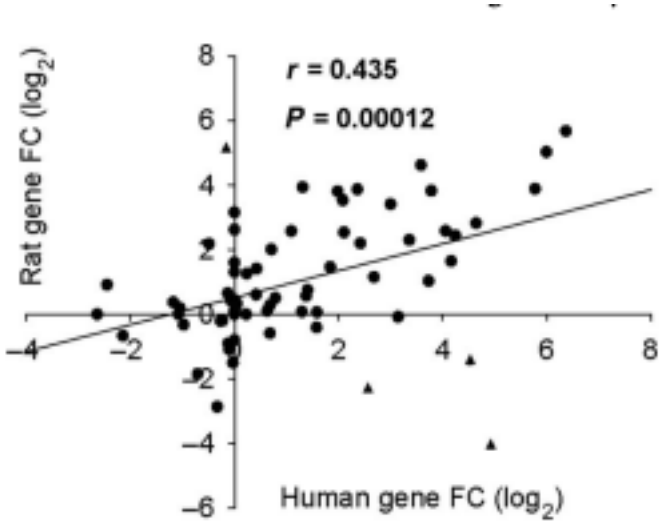

Figure 2. Correlation of UVB-induced chemokine and cytokine expression in the human and rat. Human and rat gene expression following UVB irradiation was plotted against each other. The Pearson's correlation coefficient, r = 0.435, showed that there is a positive relationship between the two data sets. This relationship is also significant with p<0.001. Potential outliers (▲, see results), n=73.

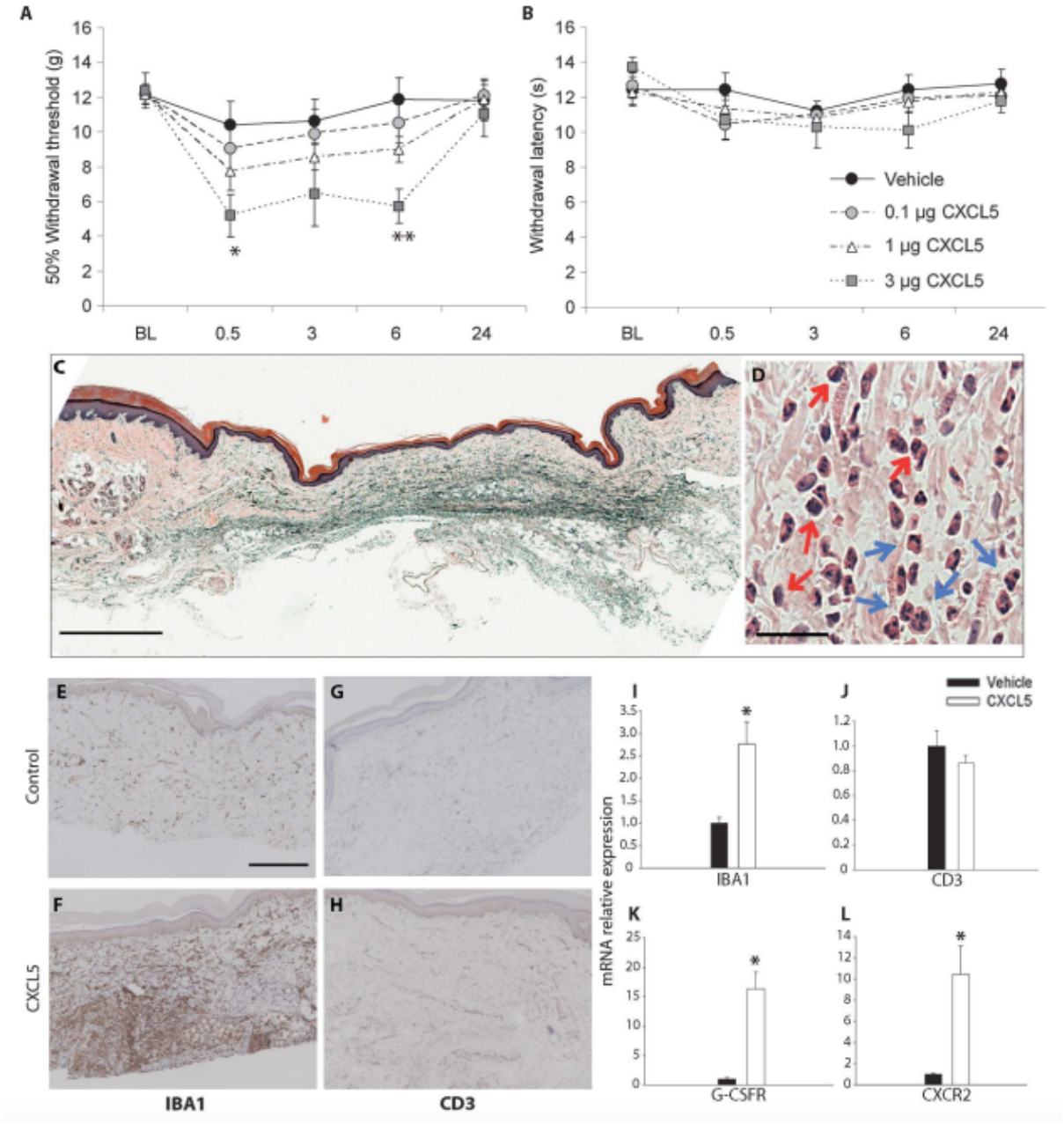

Figure 3. The chemokine CXCL5 causes mechanical pain-related hypersensitivity and induces an infiltration of neutrophils and macrophages. (A) When compared to control rats, intraplantar injection of CXCL5 (3 µg) produced a significant reduction in paw withdrawal thresholds to mechanical stimulation at 0.5 and 6 hours after treatment. No significant changes were measured in mechanical thresholds at doses of 0.1 and 1 µg. (B) In the same animals no change was observed in withdrawal latencies to thermal stimulation at any dose (**p<0.001,

*p<0.05, Two-way repeated measures ANOVA, vehicle, 0.1 µg, 1 µg n=11, 3 µg n=6). (C-D) Plantar skin preparations stained with H&E showed a marked inflammatory cell infiltrate within the dermis 6 hours after intraplantar injection of CXCL5 (3 µg). A representative section at low magnification is shown in C (scale bar, 200µm). In D, a high magnification section is shown (scale bar, 25µm) and infiltrating cells, both monocytes (red arrows) and PMNs (blue arrows) are indicated. (E-F) A low level of macrophages (as shown by IBA1 staining) is seen in the dermis of control animals (E) which dramatically increases at 6 hours after CXCL5 (3µg) injections (F) (Scale bar 200µm). (I) The increase in IBA1 expression after CXCL5 injections was confirmed with Q-PCR. (G-H) Immunopositive CD3 cells (a marker of lymphocytes) were detected at low levels in control skin (G) and did not change after CXCL5 treatment (H). (J) There was no difference in the mRNA levels of CD3 in treated versus control animals. (K-L) The mRNA of the neutrophil marker G-CSFR (K) and the cognate receptor for CXCL5, CXCR2 (L), were significantly up-regulated in the chemokine treated skin compared to control. (Mann-Whitney Rank Sum test or t-test (depending on data distribution), n=3-5, data is expressed as, *p<0.05, **p<0.01). All data are presented as mean±SEM.

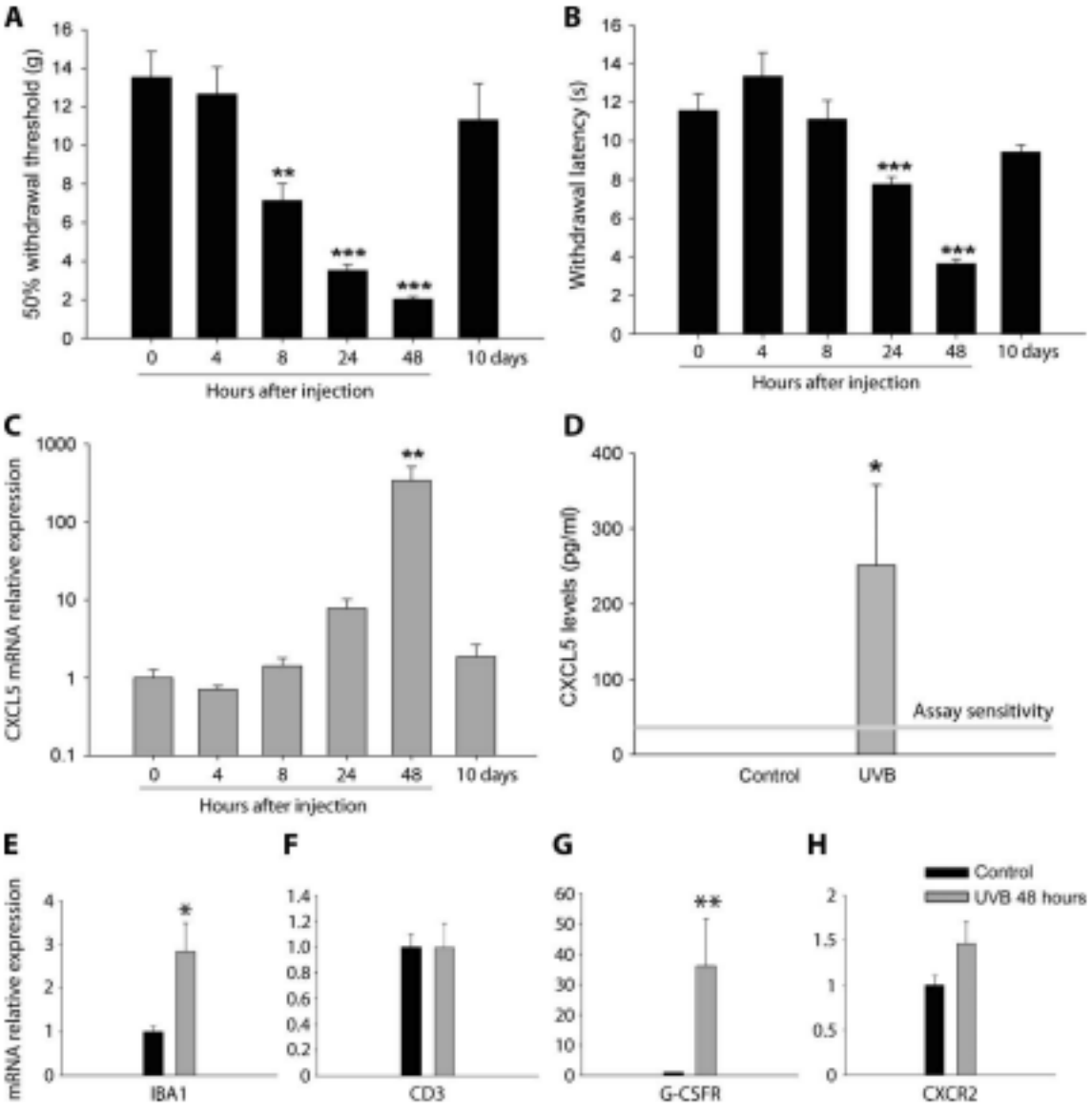

Figure 4. Time course of CXCL5 expression and pain-related hypersensitivity, in the rodent UVB model. (A-B) UVB irradiation caused a significant reduction in mechanical (A) and thermal thresholds (B) at 24 and 48 hours after treatment. Mechanical thresholds were also reduced 8 hours after UVB treatment. (C) CXCL5 mRNA expression measured at 0, 4, 8, 24, 48 hours and 10 days after 1000mJ/cm^2 of UVB. Compared to 0 hours, CXCL5 expression significantly increased at 48 hours (y-axis has a logarithmic scale). No difference was measured at other time points (Kruskal-Wallis one-way ANOVA on Ranks, n=4-5. (D) Expression of CXCL5 protein was measured with a specific ELISA. Control skin samples contained non-detectable

levels of CXCL5. However 48 hours after UVB irradiation, CXCL5 was significantly increased (n=4 per group, Mann-Whitney Rank Sum Test, p = 0.029) (E-H). UVB irradiation increased the expression of IBA1 (E) and G-CSFR (G), but not CXCR2 (H) or CD3 (F). (Mann-Whitney Rank Sum test or t-test (depending on data distribution) n=5-7, *p<0.05, **p<0.01, ***p<0.001). All data are presented as mean±SEM.

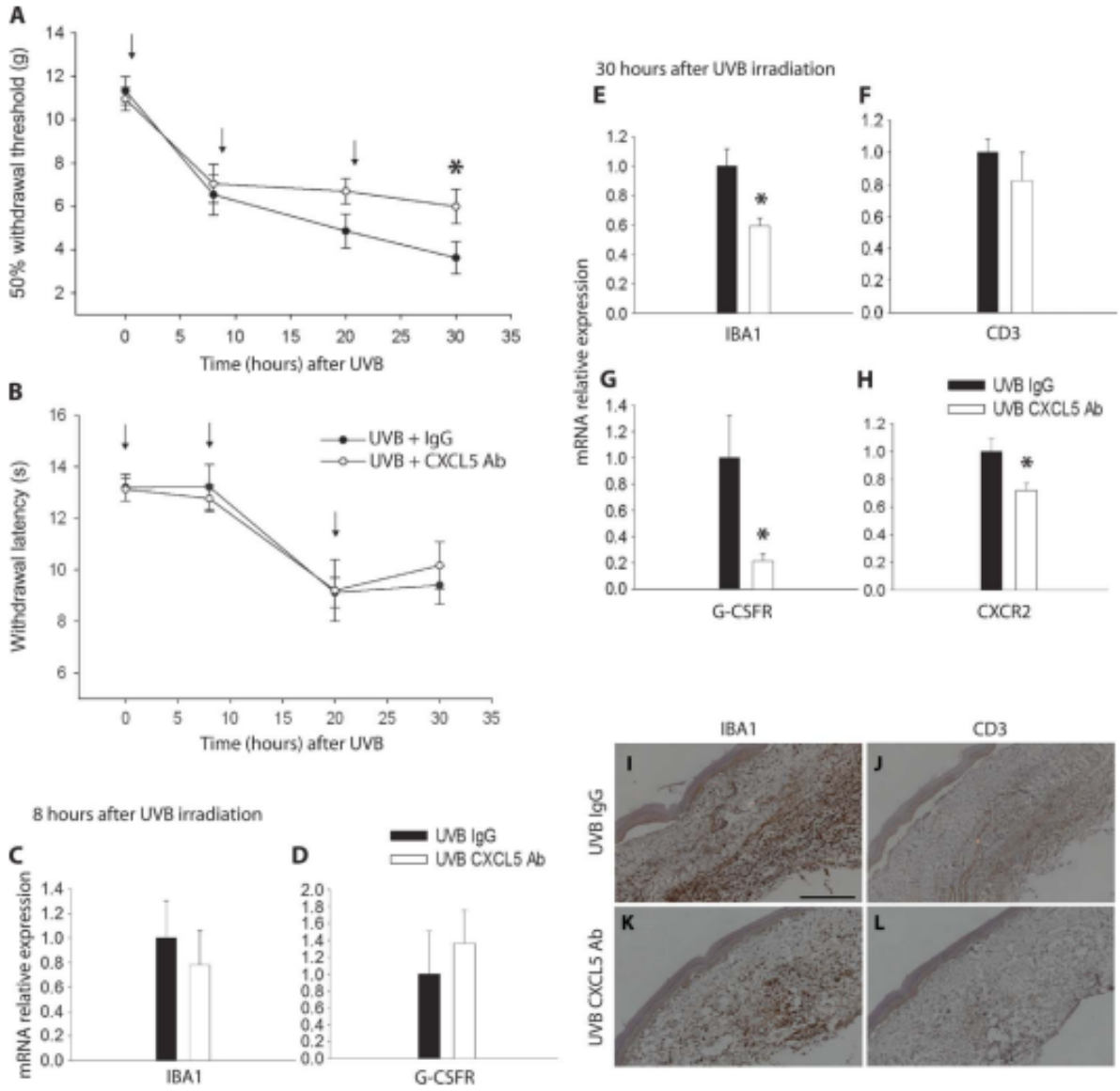

Figure 5. CXCL5 contribution to UVB-induced pain related hypersensitivity. (A-B) Animals received either a functional blocking CXCL5 antibody (Ab, 10 µg) or a control non-immune IgG (10 µg) immediately after UVB irradiation, and again at 10 and 20 hours (shown by arrows in A and B). Ab neutralisation of CXCL5 significantly attenuated the reduction in mechanical thresholds 30 hours after 1000mJ/cm^2 of UVB (A). However, neutralization of this chemokine did not have an effect on thermal thresholds after UVB irradiation (B) (Two-way repeated measures ANOVA, n=11). (C-D) At 8 hours after UVB irradiation, there was no change in infiltrating cell markers between treated and control animals. IBA1 mRNA expression was similar between CXCL5 Ab and the control IgG groups (C). Also G-CSFR mRNA expression showed no change between groups (D). (E-H) At 30 hours after UVB irradiation, a time point at which the CXCL5 neutralizing antibody is effective in decreasing hypersensitivity behaviors, there was a significant reduction in IBA1 (E), G-CSFR (G) and CXCR2 mRNA expression (H) in animals treated with CXCL5 neutralizing Ab. No difference was found in CD3 mRNA expression (F) (t-test, n=4-6, *$p<0.05$) (I-L) IBA1 staining in irradiated skin was reduced in animals treated with the CXCL5 Ab (K) versus vehicle (I). Low levels of CD3 staining were similarly detected in both groups (J, L, scale bar 200µm). All data are presented as mean±SEM.

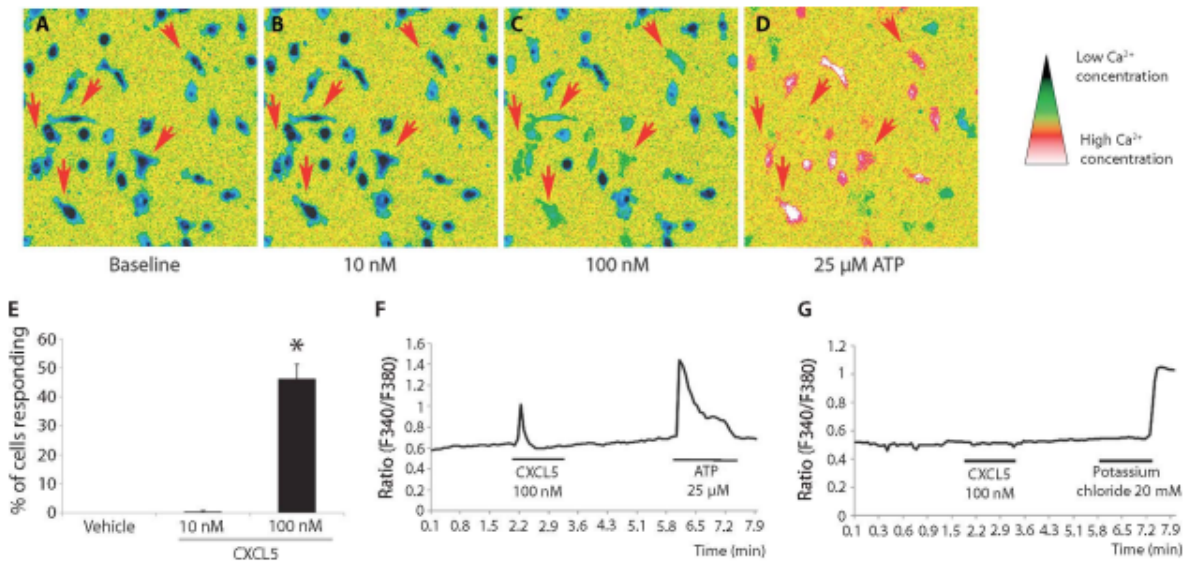

Figure 6: Exposure of macrophages to CXCL5 produced an increase in intracellular Ca^{2+} concentration $[Ca^{2+}]i$. (A-D) Macrophages in which application of ATP (25 µM) produced a change in $[Ca^{2+}]i$ (as seen in D) were included in the analysis (thus, excluding dead or non-functional cells). CXCL5 at a dose of 100nM increased $[Ca^{2+}]i$ in a number of cells as indicated by the red arrows (C). (E) The percentage of macrophages cells responding to 100nM of CXCL5 was significantly larger than after vehicle treatment (E) (Kruskal-Wallis One-way ANOVA on Ranks, n=3-6 independent experiments with at least 100 cells per concentration, data are presented as mean%±SEM). (F&G) Representative response traces of a single cell for macrophages (F) and dorsal root ganglia (DRG) neurons (G).

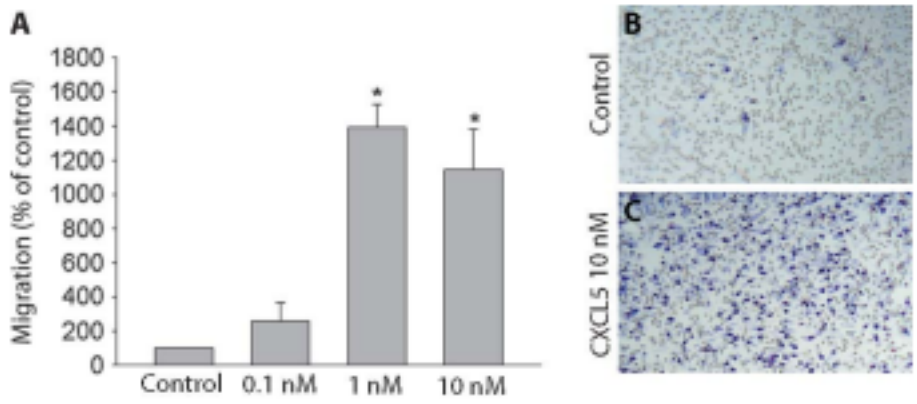

D

CXCL5 in lower wells

CXCL5 in upper wells	0	0.1 nM	1 nM	10 nM
0	100	258.5±108	* + 1392.7±133	* # 1142.9±239
0.1 nM	183.3±62	321.3±45	617.9±61	675.9±93
1 nM	297.6±71	354.1±61	504.3±37	487.7±20
10 nM	461.6±68	493.8±113	502.7±24	662.1±13

Figure 7. CXCL5 attracts cultured peritoneal macrophages. (A) When compared to control, 1 and 10nM of CXCL5 significantly increased the migration of macrophages (Kruskal-Wallis One-way ANOVA on Ranks, n=3-5). (B,C) Counterstained filters show cells in a control well (B) and a well containing 10ng/ml of CXCL5 (C). (D) To test if CXCL5 induces migration through a gradient (chemotaxis) or solely random non-directional migration (chemokinesis) we used the chequerboard analysis. In a Boyden chamber cells were suspended in increasing concentrations of CXCL5 and allowed to migrate towards increasing concentrations of CXCL5 in the lower wells. The grey boxes show the results obtained when the same concentration was used in both wells (no gradient). When there is an increasing gradient, migration is further enhanced indicating that CXCL5 induces

directional chemoattraction on macrophages (Kruskal-Wallis One-way ANOVA on Ranks, n=3-5). Significant migration across a gradient vs migration when the concentration is same,*p<0.05 compared to 0 vs 0nM, +p<0.05 compared to 1 vs 1nM, #p<0.05 compared to 10 vs 10nM). All data iare presented as the mean±SEM.

Table 1. Increase in expression of the top 20 inflammatory mediators in UVB treated skin.

Transcript levels of over 90 inflammatory mediators were measured in irradiated and non-irradiated skin, at the peak of sensory changes using custom made Taqman array cards in both the human and rat model. The level of significance was determined by t-tests comparing irradiated versus control skin for each species. Due to multiple testing p values were adjusted using the FDR. *p<0.05, **p<0.01, ***p<0.001. FC=UVB/Control. Data expressed as mean FC±SD, n=8. † validated with individual Q-PCR. ND (not detected).

Table 2. Primer sequences used in individual Q-PCR.

Table 1.

Gene Name	FC in Rat	FC in Human
CXCL5	**51.3** (20.5-128.2)*** †	**82.5** (45.4-150.0)***
iNos	**34.3** (3.1-385.1)*	**-1.1** (-2.2-1.8)
IL24	**32.7** (8.3-128.8) ***†	**63.7** (44.5-91.3)***
CXCL2	**24.6** (3.1-198.4)** †	**12.0** (8.0-18.0)***
CCL4	**15.4** (6.6-35.8)*** †	**2.5** (1.4-4.5)*
IL6	**14.8** (4.1-53.9)**	**54.7** (30.3-99.0)***
CCL2	**14.6** (5.3-40.6)***	**5.1** (3.8-7.0)***
CCL7	**14.2** (6.2-32.6) ***†	**13.8** (4.2-44.8)***
CXCL7	**14.0** (2.8-70.5)**	**4.0** (1.8-8.6)
CCL11	**11.6** (5.9-22.9)*** †	**4.2** (1.1-16.6)
IL10	**10.7** (5.4-21.2)***	**8.0** (4.1-15.8)***
IL3	**9.0** (3.4-23.3)**	ND
GCSF	**7.1** (-1.2-62.2)	**25.0** (10.7-58.5)***
IL19	**6.2** (3.0-12.6)**	ND
CCL3	**6.0** (2.9-18.9)**	**16.6** (10.7-25.7)***
CXCL4	**6.0** (3.9-9.2)***	**2.1** (-1.1-5.0)
KGF	**5.8** (3.2-10.5)***	**4.3** (2.9-6.5)***
CXCL1	**5.4** (1.9-15.5)**	**18.9** (12.6-28.4)***
IL1b	**5.0** (1.3-18.7)*	**10.3** (5.9-17.8)***
COX-2	**4.6** (2.0-10.6)**	**5.3** (3.0-9.5)***

Table 2.

Gene	Direction	Sequence (5'>3')
GAPDH	Forward	ATGGGAAGCTGGTCATCAAC
	Reverse	CCACAGTCTTCTGAGTGGCA
IBA1	Forward	TCCCCACCTAAGGCCACCAGC
	Reverse	CGTCTCCTCGGAGCCACTGGA
CD3	Forward	TTGAAGAACGAGCAGCTGTATCA
	Reverse	CGGCTGTACTGGGCATCAT
CXCL2	Forward	CACCTCCACACTGTGATAGAGATTGG
	Reverse	ATAACAGTCGTCCCGCCCTTCT
CXCL5	Forward	GCATTTCTGCTGCTGTTCACACT
	Reverse	GGTTAAGCAAACACAGCGTAGCT
CCL4	Forward	CATCGGAACTTTGTGATGGA
	Reverse	CATACTCATTGACCCAGGGC
CCL7	Forward	CTCCAAAGCCCTGAAGACAG
	Reverse	GTTCCTACCCCTTAGGACCG
CCL11	Forward	CTGCTGCTTTACCATGACCA
	Reverse	GACCCACTTTTTCTTGGGGT
IL6	Forward	TCTCTCCGCAAGAGACTTCC
	Reverse	CCGGACTTGTGAAGTAGGGA
IL24	Forward	TCTGCAGAATGTCTCGGATG
	Reverse	AGGAAGTTATCCGGATTGGC
G-CSFR	Forward	GGAGGGCTGCGGGCAAATCA
	Reverse	GGGACCCGTCAGGCAGGTGA
CXCR2	Forward	GGCCATCGTCCACGCCACAA
	Reverse	AAGATGACCCGCATGGCCCG